OATAO

Open Archive Toulouse Archive Ouverte

Open Archive Toulouse Archive Ouverte (OATAO)

OATAO is an open access repository that collects the work of Toulouse researchers and makes it freely available over the web where possible

This is an author's version published in: **http://oatao.univ-toulouse.fr/24500**

Official URL: https://doi.org/10.1016/j.jallcom.2016.09.028

Physical properties of highly crystalline CIS layer prepared using single phase electrodeposition and low temperature RTP annealing

H. Saidi [a, *], M.F. Boujmil [a], B. Durand [b], M. Bouaïcha [a]

[a] *Laboratoire de Photovoltaïque, Centre de Recherches et des Technologies de l'Energie, Technopole de Borj-Cédria, BP 95, Hammam-Lif, 2050 Tunis, Université de Tunis El Manar, Tunisia*
[b] *CIRIMAT, CNRS, INPT, Universite de Toulouse, 118, Route de Narbonne, 31062 Toulouse Cedex 9, France*

ARTICLE INFO

ABSTRACT

$CuInSe_2$ nanoparticles (CIS NP) were synthesized on ITO coated glass substrate by electrodeposition and rapid thermal processing (RTP). The as deposited films were annealed under argon atmosphere at 250 °C, 350 °C and 450 °C using RTP during a short annealing time. The latter is practicable to avoid further losing of the Se content in CIS films. In order to analyze the effect of annealing temperature, the structural, morphological, optical and electrical properties were investigated by means of X ray diffraction, scanning electron microscopy, UV Visible Spectroscopy and Mott Schottky plots respectively. XRD results show that elaborated films have a tetragonal chalcopyrite CIS with preferential orientation along the (112) orientation. The phase formation of CIS NP with good crystallinity was observed at low annealing temperature. Optical absorption studies indicate a direct band gap around 1.02 eV at 250 °C. The optical constants such as refractive index $n(\lambda)$ and extinction coefficient $k(\lambda)$ were estimated using an appropriate optical model. To determine the doping type of elaborated semi conductor, its flat band potential and the free carrier concentration we used the Mott Schottky plots. A new attempt to anneal the electrodeposited CIS films by short annealing duration using RTP process was proved to be a useful method to synthesize polycrystalline CIS films for solar cell application.

1. Introduction

Photovoltaic devices are receiving growing interest in both in dustry and research institutions due to the great demand for clean and renewable energy. Chalcopyrite $CuInSe_2$ (CIS) has become one of the most important semiconductor materials in developing polycrystalline thin films of solar cell structures mainly due to its high optical absorption coefficient ($\sim 10^5$ cm^{-1}), direct band gap (1.04 eV), long term optoelectronic stability and proper charge densities [1,2]. Moreover, this ternary semiconductor material can be prepared to have either n or p type conductivity, depending on the synthesis method and the composition of the constituent ele ments in the structure [3]. Therefore this easy conversion between n and p carriers types permits to prepare from this semiconductor homojunction and heterojunction solar cells [4]. A solar cell effi ciency of 21% has been recently obtained using CIS films as absorber layer [5,6]. A variety of physical and chemical techniques have been employed to fabricate this material. Ranging from direct evapora tion of all the elements [7], sputtering of the cations which then react with chalcogens [8], spray pyrolysis [9] and electrodepostion [10,11].

A lot of works published about chalcopyrite materials have used the one step electrodeposition process instead of physical vapor deposition because it allows achievement of low production cost, higher deposition speed and negligible waste of chemicals [12]. Nevertheless, undesirable secondary phases may be formed with chalcopyrite phase in CIS electrodeposited films such as $Cu_{2-x}Se$, In_2Se_3 [13,14]. These secondary phases are the source of high electrical resistance [11] which decreases the power conversion efficiency of the CIS solar cells. The as electrodeposited CIS pre cursor material is amorphous (nanocrystallized), thus an annealing step is necessary to promote grain growth and consequently the formation of effective absorbers. Films annealed in vacuum, nitro gen or argon atmospheres usually present high levels of Se va cancies because of the low vapor pressure of Selenium, [15,16]. To replace the lost amount of selenium and adjust the stoichiometry of the film, a thermal annealing in Se atmosphere (selenisation) was investigated [17,18]. Several works have studied the effects of

* Corresponding author.
E-mail address: houdasaiidi@yahoo.fr (H. Saidi).

classical annealing temperature and annealing time on the crystallization, composition, morphology, optical and electrical properties of CIS thin films. They showed that the formation of tetragonal chalcopyrite CuInSe$_2$ with high crystallinity quality and without secondary phases was obtained from high annealing temperature (more than 400 °C) and during an hour at least [19,20]. The rapid thermal processing (RTP) is typically carried out for short annealing periods. These suitably short durations allow substantially the diffusion of selenium to the layer of CuInSe$_2$ as well as obtaining the desired composition in the thin layer of semiconductor to improve the photovoltaic properties and mainly the adjusted band gap. As a result, the crystallinity of CIS layers is closely related with the thermal annealing process and annealing time. The purpose of this work is to show how interesting physical properties of CuInSe$_2$ films can be achieved with RTP treatment (annealing temperature) at only 250 °C. X ray diffraction (XRD), UV–Vis transmission measurements and scanning electron microscopy (SEM) techniques are used to characterize structural, morphological and optical properties of these synthesized CIS thin films, respectively.

2. Experimental details

2.1. Materials preparation

A conductive indium tin oxide coated glass substrate (ITO) of 1.5 × 1.5 cm^2 dimension was used as substrates. The latter were ultrasonically cleaned with acetone, ethanol and deionized water during 10 min. The CIS films have been electrodeposited on cleaned ITO glass substrate. The electrodeposition technique has been carried out potentiostatically using an Autolab potentiostat/galvanostat PGSTAT 30 (Eco Chemie BV) connected to a three electrode cell (K0269A Faraday Cage, Par).

The used working electrode was ITO coated glass substrate, the reference electrode was an Ag/AgCl (3 M NaCl) and a platinum plate was used as a counter electrode. The composition of the deposition bath consisted of 3 mM of InCl$_2$, 3 mM of CuCl$_2$ (2H$_2$O), 6 mM of SeO$_2$ and 0.1 M of the sodium citrate which was chosen to be a complexing agent in deionized (DI) water. The pH of the solution has been adjusted to 2 by adding HCl. The cathodic potential and deposition time have been fixed at 850 mV and 15 min, respectively. Afterwards, the samples were rinsed under DI water and dried in 60 °C oven for 10 min. Due to the amorphous nature of as deposited films and in order to improve their crystallinity, all as deposited films have been annealed in argon atmosphere at 250 °C, 350 °C and 450 °C during 5 min with a rapid thermal process (RTP) using IR heating lamps. To minimize the exhausting of the selenium from samples, it was necessary to stabilize the temperature for 10 min for each increasing of 50 °C until the final temperature [21]. The heating rate for all annealing temperatures was fixed at 5 °C/min.

2.2. Characterization

The crystal phase of the CIS films was analyzed using an X ray diffractometer (automated Bruker D8 advance) with CuK$_\alpha$ (λ 1.540 Å) radiations in the 2θ range of 10°–80°. A comparison with the Joint Committee on Powder Diffraction Standards (JCPDS) card was done for the identification of the observed peaks. The band gap energy (E$_g$) and the absorption coefficient (α) were calculated from the reflection R(λ) and transmission T(λ) spectra. The latter were measured at normal incidence with an UV–visible NIR LAMBDA 950 spectrophotometer in the wavelength domain ranging between 250 and 2200 nm at room temperature. Surface morphology of the CIS films was observed by Scanning Electron

Microscope (SEM, JEOL JSM 6700), with an accelerating voltage of 15 kV. The chemical composition of the synthesized CIS films was analyzed by The Energy Dispersive Spectroscopy (EDS) measurements. Mott–Schottky plots were carried out in the range of 1 to 0.4 V (vs. Ag/AgCl) reference electrode under a frequency of 1 kHz. This electrochemical measurement was released in an electrolyte solution of 0.5 M for Na$_2$SO$_4$ (pH 6.5) [22].

Thicknesses of electrodeposited films are theoretically evaluated using the following formula [23,24].

$$d \quad \frac{1}{n\,F\,A}\left(\frac{i\,t\,m}{\rho}\right) \tag{1}$$

where: F 96,500 C is the Faraday constant, A is the electrode area, i is the applied current, t is the deposition time, M 336.28 g mol^{-1} is the CIS molecular weight and the density of CIS material is equal to 5.77 g cm^{-3} [25].

The number of electrons necessary for depositing one molecule of stoichiometric CIS is taken 13 according to the overall following reaction in the electrochemical cell [26]:

$$Cu^{2+} + In^{3+} + 2SeO_3^- + 12\,H^+ + 13\acute{e} \rightarrow CuInSe_2 + 6H_2$$

Obtained thickness is about 1.02 μm. It corresponds to the layer before RTP annealing and is used as initial value in the fitting procedure of section 4.

3. Results and discussion

3.1. Structural analysis

Fig. 1 shows XRD patterns recorded for CIS thin films grown onto ITO – coated substrates under different annealing temperature (250 °C, 350 °C and 450 °C) with RTP during 5 min. For the as deposited films, in addition to the ITO diffraction peaks, we note the appearance of two diffraction peaks at approximately 26.85° and 44.35° assigned respectively to the miller indices (112) and (204)/(220) of the ternary CIS. This result provides the beginning of the formation of the CIS's seed with poor crystallinity [27].

After RTP annealing, the diffraction peaks observed for CIS films treated at 250 °C, 350 °C and 450 °C, revealed that all films were polycrystalline in nature of chalcopyrite structure with preferential
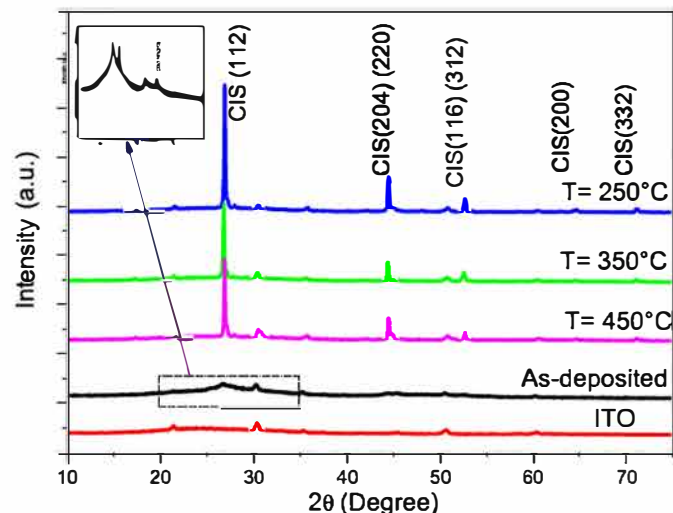

Fig. 1. XRD patterns of electrodeposited CIS layers onto (ITO)-coated glass substrate treated at various annealing temperature.

orientation along the (112) direction. The main diffraction peaks observed at 26.80°, 44.55° and 52.60° are assigned respectively to the (112), (204)/(220) and (116)/(312) plans. This was verified by JCPDS database with cards number 0040 1487. The peak (112), suitable for photovoltaic cell, was observed in all films [28]. By increasing the annealing temperature, the intensity of the main peak (112) increases. Indeed, the sample annealed at 250 °C had the maximum of (112) peak intensity. Whereas at 350 °C and 450 °C, the full width at half maximum (FWHM) of the most intense peaks become narrow and favorites the (112) preferential orientation. On the other hand, as shown in Fig. 1, the FWHM of the main peaks (112) is found to decrease when the annealing temperature rises. Thus we obtained FWHM values of 2.31°−0.13° 0.12°−0.11°, for as deposited film and 250 °C 350 °C 450 °C, respectively. This in dicates that the crystalline nature of the CIS films improves when the RTP annealing temperature rises. Comparing the crystallization of as deposited films, as shown in inset graph of Fig. 1, and after RTP annealing, we can conclude that the relatively short annealing time with this process improved the crystallization of the CuInSe$_2$ pha ses. We also note that no peaks related to secondary phases such as CuSe$_2$, In$_2$Se$_3$, etc, are observed in all diffractograms. Several in vestigations [14−29] have been reported on the presence of binary phase such as Cu Se and In Se with the formation of CIS thin films even at high annealing temperature.

In order to measure the degree of preferential orientations in the CIS films, we used the variable R$_{I(hkl)}$, defined in equation (2) as the ratio of the major peak (112) intensity to the sum of the in tensities of all peaks presents in the X ray patterns [28].

$$R_{I_{(hkl)}} \quad \frac{I_{(hkl)}}{\sum I_{(hkl)}} \tag{2}$$

where I $_{hkl}$ is the intensity of a sole (hkl) peak.

On the other hand, a complete (hkl) texture of the layer would lead to R 1. For information, the R$_{(112)}$ of a non textured powder estimated from JCPDS data is about 0.3 [30]. Values of preferential orientations R$_{(112)}$ of CIS samples prior and after annealing are lis ted in Table 1. It shows that the texturisation coefficient remains constant and equal to 0.70 with increasing annealing temperature. This result indicates that the thin film has been preferentially ori ented towards (112) reflection. Otherwise, this orientation is more adequate to photovoltaic applications.

The plane spacing d is calculated from the (112) and (220) reflection peaks according to Bragg's formula (3):

$$d_{(hkl)} \quad \frac{n\lambda}{2 \sin \theta} \tag{3}$$

where d$_{(hkl)}$ is the inter planar spacing, θ refers to Bragg angle and λ is the K$_{\alpha 1}$ wavelength (λ 1.540 Å).

The lattice constants for chalcopyrite semiconductor materials of tetragonal symmetry are given by the following formula.

$$\frac{1}{d_{hkl}^2} \quad \frac{h^2 + k^2}{a^2} + \frac{l^2}{c^2} \tag{4}$$

The lattice constants of elaborated films are listed in Table 2. We show that the two lattice parameters a and c range from 5.75 to 5.78 Å and 11.37 Å to 11.57 Å, respectively. These values are in good agreement with those reported in the JCPDS files [30].

❖ **Grain size**

The crystallite size (D) of the CIS through (112) orientation has been evaluated by the Scherrer's formula expressed as (5) [31,32]:

$$D \quad \frac{k\lambda}{\beta \cos \theta} \tag{5}$$

where λ is the wavelength of CuKα line (λ 1.540 Å), β is the values of the FWHM of (112) peak and θ is the Bragg angle.

The calculated values of the crystallite size are show in Fig. 2. We notice that for the as deposited film, the average crystallite size of CIS film is in the order of 4 nm.

After RTP annealing, we found that the crystallite size was increased when the annealing temperature increases. Obtained values are 61 nm, 64 nm and 71 nm for 250 °C, 350 °C and 450 °C annealing temperatures, respectively.

3.2. Morphological and compositional analysis

In Fig. 3 we give SEM images of the as deposited and annealed CIS layers at different temperatures for 5 min with RTP, including 250 °C, 350 °C and 450 °C. We notice a change in the surface morphology. Therefore, micrograph (Fig. 3a) shows non uniform grain sizes and non homogeneous surface with mixture of smaller and larger clusters. After annealing at 250 °C (Fig. 3b), we observe that the surface of the film becomes smoother and has a more uniform grain size distribution. When the annealing tem perature increases, especially at 450 °C (Fig. 3d), the surface morphology is deteriorated displaying grains/particles with uneven sizes.

SEM results and XRD analysis show that treated film with RTP at low annealing temperature (T 250 °C) have improved crystalli zation properties.

The chemical compositions of the CIS layer annealed at 250 °C with RTP during 5 min were analyzed by EDS. The results of the compositional analysis of sample are summarized in Table 3 and Fig. 4. One can observe the presence of copper, indium and sele nium elements in this film (250 °C) as obtained in XRD analysis. Other elements such carbon, oxygen and silicon are attributed to the glass substrate and residual nitrogen may be due to used chemical agents. In addition, this sample contains Se in excess, with

Table 2
Chemical composition of the synthesized layer treated at T 250 °C.

Element	Wt%	At%
Cu$_K$	17.19	22.52
Se$_L$	52.99	55.87
In$_L$	29.64	21.49
Sn	0.17	0.12
Totals	100	

Table 1
XRD parameters obtained for electrodeposited CuInSe$_2$ thin films through (112) orientation as a function of annealing temperature.

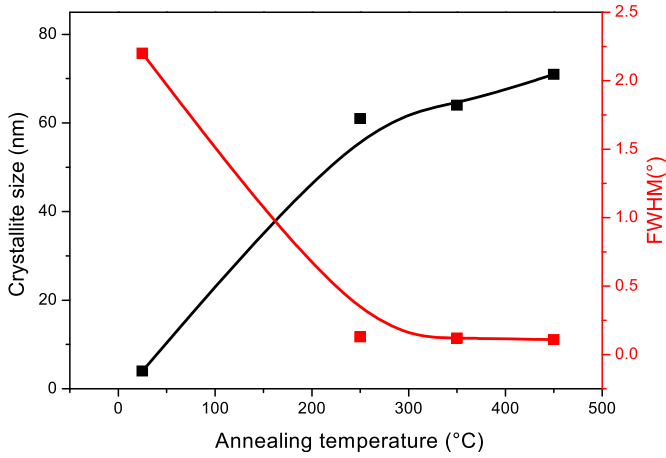| Annealing temperature T (°C)	Bragg angle 2θ(°)	FWHM (°)	Grain size D (nm)	a (A°)	c (A°)	R $_{I(112)}$
As-deposited	26.67	2.31	4	5.78	11 43	0.70
250	26.92	0.13	61	5.75	11.40	0.70
350	26.83	0.12	64	5.77	11.57	0.70
450	26.91	0.11	71	5.76	11.37	0.70

Fig. 2. Average crystallite size D (nm) and FWHM for the (112) CIS peak for different annealing temperatures.

3.3. Optical properties

The absorption coefficient (α) was calculated from the mea surements of optical transmittance $T(\lambda)$, reflectance $R(\lambda)$ and film thickness (d) using the formula (6) [33].

$$\alpha = \frac{1}{d} \ln \left[\frac{(1 - R)^2}{T} \right] \qquad (6)$$

Besides, it is well known that CIS is a direct band gap semi conductor. The absorption coefficient, α, is related to energy gap, E_g, according to the following formula [34]:

$$\alpha h\nu = B (\alpha h\nu - E_g)^{1/2} \qquad (7)$$

where $h\nu$ is the incident photon energy, h is the Planck constant and B is a constant.

The optical band gap of films has been evaluated using Tauc's method by plotting $(\alpha h\nu)^2$ versus $h\nu$ as illustrated in Fig. 5 where
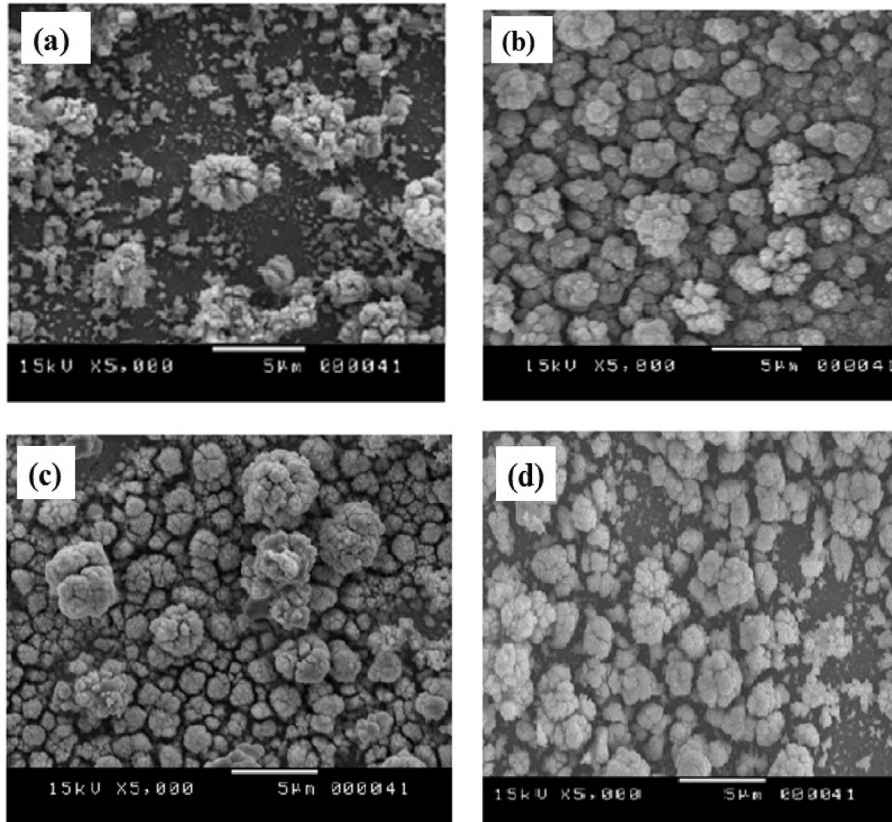

Fig. 3. SEM micrographs of CIS films: (a) as-deposited, (b) annealed at 250 °C, (c) T = 350 °C and (d) T = 450 °C during 5 min.

an atom% of about 56%. Consequently, 250 °C is an adequate RTP annealing temperature that kept Se.

Table 3
Mott-Schottky parameters of the CIS films with different annealing temperature in Na$_2$SO$_4$ electrolyte.

Annealing temperature T (°C)	V$_{fb}$ (V)	N$_A$ (x 10^{17}cm^{-3})	Type
250	0.05	15.00	p
350	0.20	4.43	p
450	0.30	3.40	p

we extrapolate the linear portion of the absorption edge with en ergy axis. We found that when we increased the annealing tem perature, the direct band gap energy decreases from 1.02 eV to 0.94 eV. The gradual decrease of E_g with the annealing temperature is shown in inset graph of Fig. 5. This reduction could be explained by the rearrangement of atoms in the crystalline lattice and the decrease of the defects in microstructure [35].

Values of obtained band gap energies in this work are favorable for absorption of the long wavelength photons (NIR) in the solar spectra and are in good agreement with those presented in
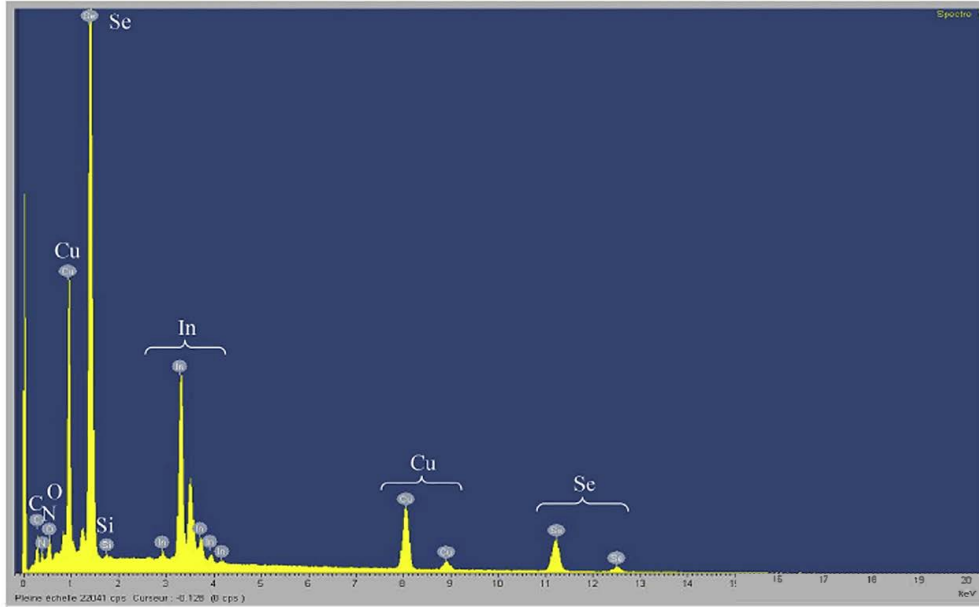
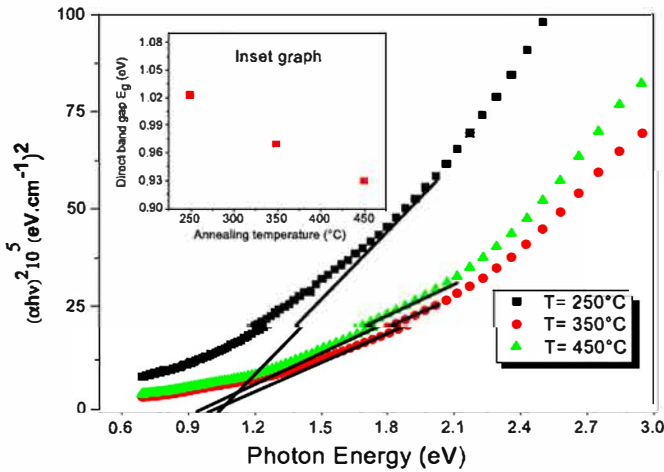Fig. 4. The composition analysis obtained by EDS of the CIS film annealed at 250 °C.

Fig. 5. Plots of $(\alpha h\nu)^2$ vs. photon energy ($h\nu$), for the CuInSe$_2$ thin films at various annealing temperatures measured by UV spectrum.

previous works [35,36]. Moreover, the optimum value of E_g (~1.02 eV) is due to the formation of a single phase of the ternary CIS as shown after treatment in RTP at low temperature (250 °C). This conclusion is confirmed by XRD analysis.

3.4. Electrical properties

The Mott–Schottky (M S) analysis is usually used to evaluate the relationship between the space charge layer capacitance and flat band potential (V_{fb}) based on equation (8) [37]:

$$\frac{1}{C_{sc}^2} \quad \frac{2}{\varepsilon\varepsilon_0 eS^2 N}\left(\pm\left(V \quad V_{fb}\right) \quad \frac{KT}{e}\right) \qquad (8)$$

where, C, e, S, K and T are the capacitance of the space charge layer, the elementary charge, the surface area, the Boltzmann constant and absolute temperature, respectively. Whereas ε is the dielectric constant of the semiconductor, ε_0 is the electrical permittivity of vacuum. V is the applied voltage, N stands for the density of donor (N_D) or acceptor (N_A) and V_0 is the built in potential in the semi conductor which is about the potential across the depletion region in thermal equilibrium.

The shape of the M S plot provides information on the con ductivity type of the semiconductor, where, negative slope is for p type and positive one is for n type semiconductor. In the other hand, value of the free charge carrier concentration can be deter mined from the slope of $1/C_{sc}^2$ vs. V plot and V_{fb} can be obtained by extrapolation to the intercept of the potential axis ($1/C_{sc}^2$ 0). Fig. 6 shows the M S plot for the CIS in 0.5 M Na$_2$SO$_4$ electrolyte at 250 °C, 350 °C and 450 °C. It can be seen that the plot has a negative slope, as expected for a p type CIS films. Also, as shown in Table 3, both values of V_{fb} and N_A are changed by varying the annealing tem perature. In fact, the estimated flat band potentials V_{fb}, corre sponding to the position of the valence band, increases from 0.05 V to 0.30 V with the increase of the annealing temperature. Whereas the carrier density was found to be in the range of $1.5 10^{18}$ cm^{-3}–$3.4 10^{17}$ cm^{-3} and can decrease by increasing the annealing temperature. Variations of V_{fb} and N_A are likely to depend on the surface states, the composition of elements in films and the syn thesis methods.

4. Optical modeling

The optical parameters, such as refractive index n(λ), extinction coefficient k(λ) and band gap energy of the CIS films were extracted from the experimental curves of reflection R(λ) and transmission T(λ) using a fitting program (Matlab). For this purpose we have used the Fresnel matrix (S) applied to the model of thin films.

This model consists of considering multilayered films formed by N planar layers, parallel, homogeneous and isotropic, characterized by a complex refractive index n$_i$. Expression of the transmission of a wave propagating at normal incidence through these multilayered films can be determined using the Jones formalism [38]. In studying the reflected and transmitted fields at each interface of the system, the amplitudes at the input and the output of the system are related by the following equation:
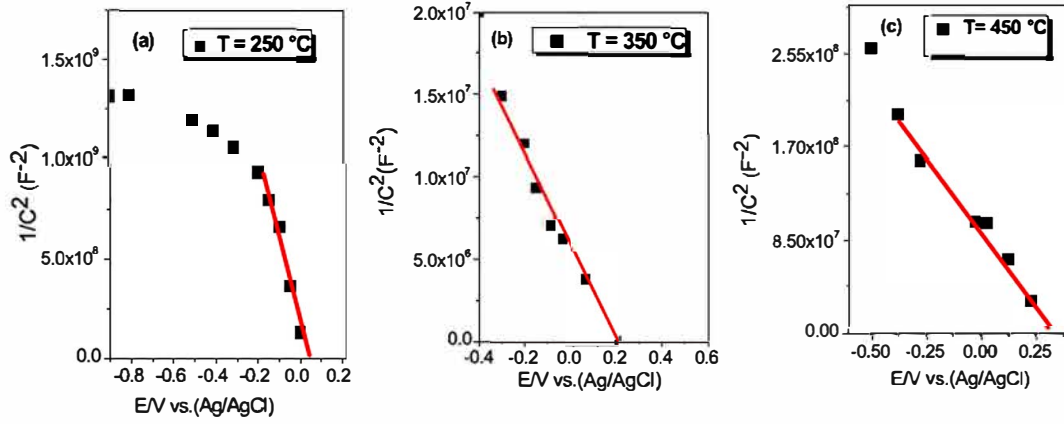
Fig. 6. Mott-Schottky plots for CIS layers in 0.5 M Na$_2$SO$_4$ annealed at different temperatures: (a) T = 250 °C; (b) T = 350 °C and (c) T = 450 °C.

$$\begin{pmatrix} E_0^+ \\ E_0^- \end{pmatrix} = S \begin{pmatrix} E_{N+1}^+ \\ 0 \end{pmatrix} \tag{9}$$

where E_0^+ and E_0^- are the incident and the reflected fields at the entrance of the system, respectively, and E_{N+1}^+ is the output transmitted field. The Fresnel matrix S is the product of the transfer matrices associated with each layer expressed in terms of their individual reflectance r_i and transmittance t_i coefficients (Fresnel coefficient) at each interface (I_i). It's as shown in these following equations:

$$S = \prod_0^{N-1} I_k L_{k+1} \tag{10}$$

Thus:

$$S = \begin{pmatrix} S_{11} & S_{12} \\ S_{21} & S_{22} \end{pmatrix} \tag{11}$$

$$I_i = \frac{1}{t_i} \begin{pmatrix} 1 & r_i \\ r_i & 1 \end{pmatrix} \tag{12}$$

$$L_i = \begin{pmatrix} e^{-i\beta_i} & 0 \\ 0 & e^{i\beta_i} \end{pmatrix} \tag{13}$$

$$r_i = \frac{n_i - n_{i+1}}{n_i + n_{i+1}} \tag{14}$$

$$t_i = \frac{2\tilde{n}_i}{\tilde{n}_i + \tilde{n}_{i+1}} \tag{15}$$

The global reflection and transmission coefficients as a function of matrix' coefficients are given by:

$$r_c = \frac{S_{21}}{S_{11}} \tag{16}$$

$$t_c = \frac{1}{S_{11}} \tag{17}$$

Expressions of reflectance and transmission coefficients can be calculated according to the following formulas:

$$R = |r_c|^2 \tag{18}$$

$$t_c = \frac{n_{N+1}}{n_0} |t_c|^2 \tag{19}$$

In our case, the multilayer contains three layers. The latter is air/CIS/ITO/glass/air having complex refractive indexes and thicknesses (n_1, d_1), (n_2, d_2) and (n_{sub}, D), respectively. n_0 is the refractive index of air.

Consequently, the new term of the Fresnel matrix is given by this equation:

$$S = I_0 L_1 I_1 L_2 I_2 L_3 \tag{20}$$

$R(\lambda)$ and $T(\lambda)$ spectra of CIS layers after RTP annealing at 250 °C are plot in Fig. 7. One can deduce that the film has low transmission values in the visible range and reaches about 25% at 850 nm. Whereas, the reflection spectrum has very low values in the 400–1600 nm domain, but rises after 1800 nm. This result confirms that the elaborated chalcopyrite CIS layer with an RTP treatment is a good absorber.

The theoretical values of the refractive index $n(\lambda)$ and the extinction coefficient $k(\lambda)$ as depicted in Fig. 8 were determined
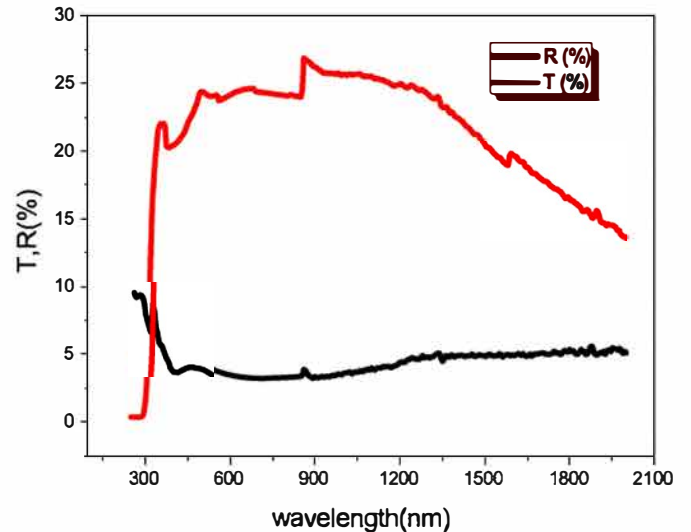

Fig. 7. Measured transmission and reflection spectra of CuInSe$_2$ film annealed at 250 °C.
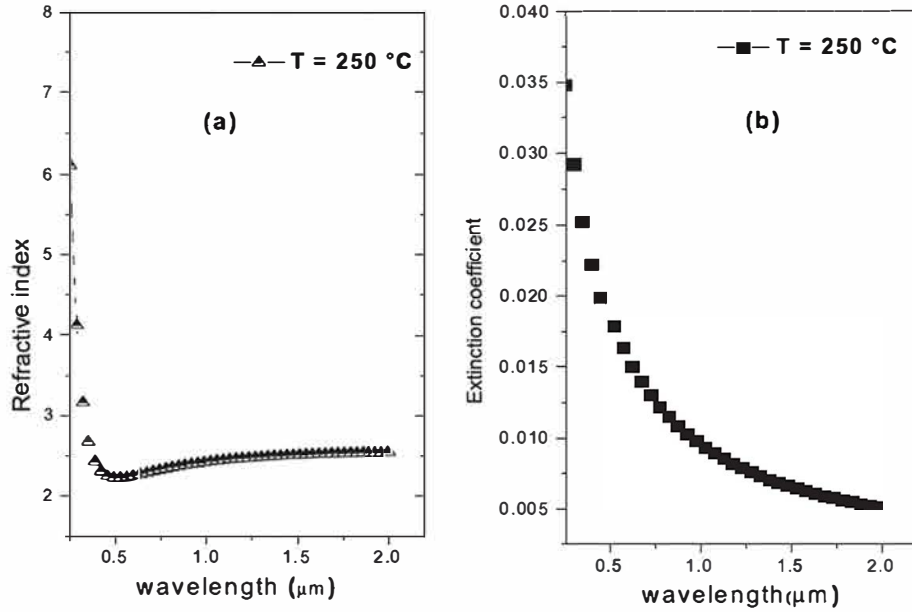
Fig. 8. Optical parameters: (a) refractive index, n, and b extinction coefficient, k, vs. wavelength for CuInSe₂ thin films (annealed at 250 °C for 5min).

using the Cauchy model. These optical parameters are calculated by these following expressions:

$$n \quad A+\frac{B}{\lambda^2}+\frac{C}{\lambda^4} \qquad (21)$$

$$k \quad \frac{A'}{\lambda}+\frac{B'}{\lambda^3}+\frac{C'}{\lambda^5} \qquad (22)$$

where λ is the wavelength and A, B, C, A', B' and C' are constants.

Optical parameters $n(\lambda)$, $k(\lambda)$ and band gap energy were carried out by fitting theoretical curves of $R(\lambda)$ and $T(\lambda)$ to experimental ones over the entire spectral range [250−2000 nm] as plotted in Fig. 9. As shown in this figure, the refractive index decreases with increasing wavelength, it reaches a value of about 2.4 in the near infrared range. The extinction coefficient, in turn, decreases from 0.020 to 0.005 in the spectral range [250−2000 nm].

The absorption coefficient, α, is related to the extinction coefficient by:

$$\alpha \quad \frac{4\pi k}{\lambda} \qquad (23)$$

The band gap energy was estimated from the absorption edge using the previous equation (23) which is illustrated in Fig. 10. As a result, we obtain a variation on the optical band gap from 1.10 eV to 0.94 eV when the RTP annealing temperature rises. This is in good agreement with obtained results from the transmission spectra. Obtained energies of the band gap are suitable for photovoltaic conversion in solar energy.

5. Conclusion

Highly crystalline CuInSe₂ thin films were fabricated on ITO coated glass substrates using one step electrodeposition process and RTP treatment. The effect of annealing temperature using a rapid thermal processing on the structural, morphological and
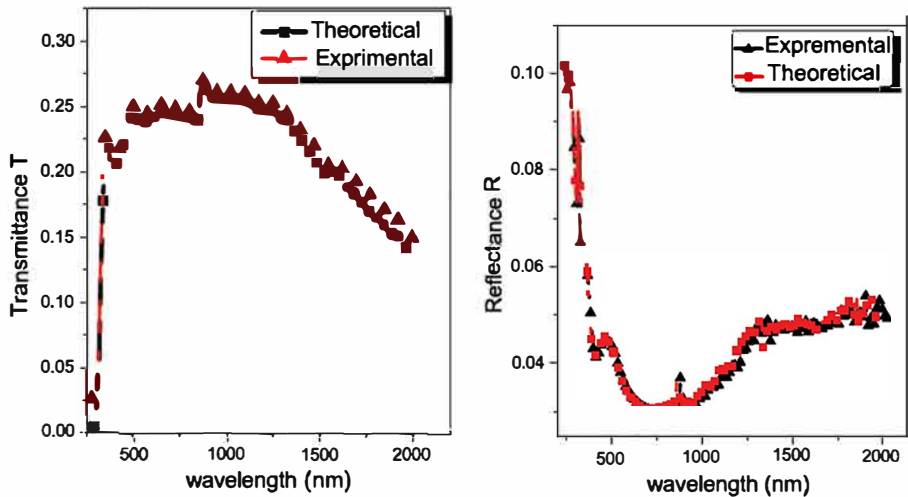

Fig. 9. Fitting results of theoretical spectra of R and T to experimental ones of CuInSe₂ thin films treated at 250 °C.
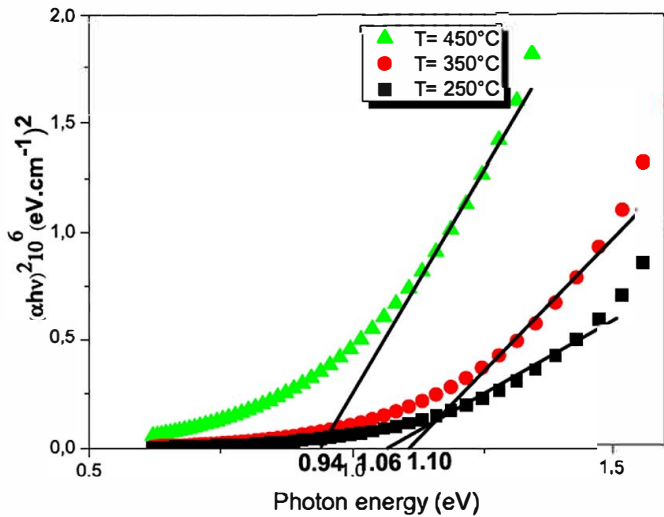
Fig. 10. Plots of $(\alpha h\nu)^2$ vs. photon energy (hν), of synthesized CIS layers at various annealing temperatures using optical modeling.

optical proprieties of CIS films was investigated.

XRD analysis shows that we obtained a single phase of the CuInSe$_2$ with good crystallinity at a low annealing RTP temperature (250 °C) having a high degree of preferred orientation towards (112) reflection. Thus, the average crystallite size of CIS NP was estimated using the Scherrer formula. It has the order of 61 nm after annealing at 250 °C. No secondary phases were observed in all films. EDS and SEM analysis confirm the presence and crystalline aspect of fabricated CIS layer when it is treated at 250 °C for a short annealing time. The flat band potential and free carrier concentrations were estimated using the Mott Schottky plots. It was found that fabricated CuInSe$_2$ film is a p type semiconductor. In the free carrier absorption zone [1000–2000 nm], the optical modeling showed that the electrodeposited CIS have a refractive index and extinction coefficient about 2.4 and 0.005, respectively. The optical band gap of CuInSe$_2$ films measured by UV spectrum is about 1.02 eV at 250 °C which is close to the band gap estimated by fitting results of theoretical spectra (1.06 eV). Obtained physical results of the CIS layer RTP annealed at 250 °C are promising for its use in solar energy.

References

[1] T. Maeda, T. Takeichi, T. Wada, Systematic studies on electronic structures of CuInSe$_2$ and the other chalcopyrite related compounds by first principles calculations, Phys. Status Solidi (A) 203 (2006) 2634 2638.

[2] A. Duchatelet, T. Sidali, N. Loones, G. Savidand, E. Chassaing, D. Lincot, 12.4% Efficient Cu(In,Ga)Se$_2$ solar cell prepared from one step electrodeposited Cu-In-Ga oxide precursor layer, Sol. Energy Mater. Sol. Cells 119 (2013) 241 245.

[3] K.L. Chopra, P.D. Paulson, V. Dutta, Thin film solar cells: an overview, Prog. Photovolt. Res. Appl. 12 (2004) 69 92.

[4] M. Kemell, M. Ritala, M. Leskela, Thin film deposition methods for CuInSe$_2$ solar cells, Crit. Rev. Solid State Mater. Sci. 30 (2005) 1 31.

[5] M.A. Green, K. Emery, Y. Hishikawa, W. Warta, E.D. Dunlop, Solar cell efficiency tables (version 47), Prog. Photovolt. Res. Appl. 24 (2016) 3 11.

[6] Powalla M, Jackson P, Hariskos D, Paetel S, Witte W, Wuerz R, Lotter E, Menner R, Wischmann W. CIGS thin-film solar cells with an improved efficiency of 20.8%. 29 th European Photovoltaic Solar Energy Conference, 3AO.4.2, Amsterdam, September 2014.

[7] M.A. Contreras, M.J. Romero, R. Noufi, Characterization of Cu (In, Ga)Se$_2$ Materials used in record performance solar cells, Thin Solid Films 51 (2006) 511 512.

[8] J. Piekoszewski, J.J. Loferski, R. Beaulieu, RF-sputtered CuInSe2 thin films, Sol. Energy Mater 2 (1980) 363 372.

[9] M. Krunks, O. Kijatkina, H. Rebane, L Oja, V. Mikli, A. Mere, Composition of CuInS$_2$ thin films prepared by spray pyrolysis, Thin Solid Films 403 404 (2002) 71 75.

[10] J.S. Wellings, A.P. Samantilleke, S.N. Heavens, P. Warren, I.M. Dharmadasa, Electrodeposition of CuInSe$_2$ from ethylene glycol at 150 °C, Sol. Energy Mater. Sol. Cells 93 (2009) 1518 1523.

[11] S. Mandati, B.V. Sarada, S.R. Dey, S.V. Joshi, Pulsed electrodeposition of CuInSe$_2$ thin films with morphology for solar cell applications, J. Electrochem. Soc. 160 (2013) 173 177.

[12] O. Meglali, N. Attaf, A. Bouraiou, J. Bougdira, M.S. Aida, G. Medjahdi, Chemical bath composition effect on the properties of electrodeposited CuInSe$_2$ thin films, J. Alloys Comp. 587 (2014) 303 307.

[13] E. Saucedo, C.M. Ruiz, E. Chassaing, J.S. Jaime-Ferrer, P.P. Grand, G. Savidand, V. Bermudez, Phase evolution during CuInSe$_2$ electrodeposition on poly-crystalline Mo, Thin Solid Films 518 (2009) 3674.

[14] S. Niki, R. Suzuki, S. Ishibashi, T. Ohdaira, P.J. Fons, A. Yamada, H. Oyanagi, T. Wada, R. Kimura, T. Nakada, Anion vacancies in CuInSe$_2$, Thin Solid Films 387 (2001) 129 134.

[15] B.M. Basol, V.K. Kapur, G. Norsworthy, A. Halani, C.R. Leidholm, R. Roe, Efficient CuInSe$_2$ solar cells fabricated by a novel ink coating approach, Electro-chem. Solid-State Lett. 1 (1998) 252 254.

[16] G. Norsworthy, C.R. Leidholm, A. Halani, V.K. Kapur, R. Roe, B.M.R. Basol Matson, CIS film growth by metallic ink coating and selenisation, Sol. Energy Mater 60 (2000) 127 134.

[17] M. Benaicha, N. Benouattas, C. Benazzouz, L. Ouahab, Effect of bath temperature and annealing on the formation of CuInSe$_2$, Sol. Energy Mater. Sol. Cells 93 (2009) 262 266.

[18] C. Guillen, J. Herrero, Improved selenisation procedure to obtain CuInSe2 thin-films from sequentially electrodeposited precurseurs, J. Electrochem. Soc. 143 (1996) 493 498.

[19] W. Deng, Z. Yan, P. Ding, Y. Wang, Y. Fang, M. Sun, Y. Su, Phase composition of CuInSe$_2$ in different annealing process, Mater. Sci. Semicond. Process 26 (2014) 419 424.

[20] Y. Shi, Z. Jin, C. Li, H. An, J. Qiu, Effects of post-heat treatment on the char-acteristics of chalcopyrite CuInSe$_2$ film deposited by successive ionic layer absorption and reaction method, Thin Solid Films 515 (2007) 3339 3343.

[21] J.F. Guillemoles, P. Cowache, A. Lusson, K. Fezzaa, One step electrodeposition of CuInSe$_2$, Improved structural, electronic, and photovoltaic properties by annealing under high selenium pressure, J. Appl. Phys. 79 (1996) 7293.

[22] A. Aghassi, M. Jafarian, L Danaee, F. Gobal, M.G. Mahjani, AC impedance and cyclic voltammetry studies on PbS semiconducting film prepared by electro-deposition, J. Electroanal. Chem. 661 (2011) 265 269.

[23] R. Friedfeld, R.P. Raffaelle, J.G. Mantovani, Electrodeposition of CuIn$_x$ Ga$_{1-x}$ Se$_2$ thin films, Sol. Energy Mater. Sol. Cells 58 (1999) 375.

[24] M. Faraday, Experimental researches in electricity series, Seventh Philos. Trans. R. Soc. 124 (1834) 77.

[25] R.C. Weast (Ed.), CRC Handbook of Chemistry and Physics, CRC, Boca Raton, FL, 1980.

[26] G.E.A Muftah, A.P. Samantilleke, P.D. Warren, S.N. Heavens, I.M. Dharmadasa, Electrochemical deposition of CuInTe$_2$ layers for applications in thin film solar cells, J. Mater. Sci. Mater Electron 21 (2010) 373 379.

[27] H. Lee, W. Lee, J.Y. Kim, M.J. Ko, K. Kim, Highly dense and crystalline CuInSe$_2$ thin films prepared by single bath electrochemical deposition", Electrochim. Acta 87 (2013) 450 456.

[28] J. Muller, J. Nowoczin, H. Schmitt, Composition, structure and optical prop-erties of sputtered thin films of CuInSe$_2$, Thin Solid Film. 496 (2006) 364 370.

[29] O. Volobujeva, M. Altosaar, J. Raudoja, E. Mellikov, M. Grossberg, L. Kaupmees, P. Barvinschi, SEM analysis and selenization of Cu In alloy films produced by co-sputtering of metals, Sol. Energy Mater. Sol. Cells 93 (2009) 11 14.

[30] International Center for Diffraction Data, ICDD, PDF2 Database, file number 40-1487 for CuInSe$_2$.

[31] B.E. Warren, X-ray Diffraction, Dover. New, York, 1990, p. 253.

[32] U. Holzworth, N. Gibson, The Scherrer equation versus the 'Debye-Scherrer equation, Nat. Nanotech. 6 (2011) 534, http://dx.doi.org/10.1038/nnano.

[33] J.C. Berned, L. Assmann, Polycrystalline CuInSe$_2$ thin films synthesized by microwave irradiation, J. Vac. 59 (2000) 885 893.

[34] M.C. Zouaghi, T.B. Nasrallah, S. Marsillac, J.C. Berned, B. Said, Physico-chemical characterization of spray-deposited CuInS$_2$ thin films, Thin Solid Films 382 (2001) 39 46.

[35] Y. Shi, Z. Jin, C. Li, H. An, J. Qiu, Effects of post-heat treatment on the char-acteristics of chalcopyrite CuInSe$_2$ film deposited by successive ionic layer absorption and reaction method, Thin Solid Films 515 (2007), 3339 33343.

[36] S. Agila, D. Mangalaraj, SaK. Narayandass, G. Mohan Rao, Effect of thickness and substrate temperature on structure and optical band gap of hot wall-deposited CuInSe$_2$ polycrystalline thin films, Phys. B 365 (2005) 93 101.

[37] J. Newman, E. Karen, T. Alyea, Electrochemical Systems, third ed., John Wiley & Sons Inc. Publication, Hoboken, N.J, 2004.

[38] E.L. Rafael, D.R. Carrera, B. Eusebio, S.H. Ruiz, Transformation matrices for the Mueller Jones formalism, Optik. 119 (2008) 757 765.